Available online at www.sciencedirect.com

ScienceDirect

Ceramics International 39 (2013) 8687–8692

CERAMICS INTERNATIONAL

www.elsevier.com/locate/ceramint

Effect of yttrium solubility on the structural and optical properties of $Bi_{1.5-x}Y_xZn_{0.92}Nb_{1.5}O_{6.92}$ pyrochlore ceramics

A.F. Qasrawi[a,b,*], A. Mergen[c]

[a]Department of Physics, Arab-American University, Jenin, West Bank, Palestine
[b]Group of Physics, Faculty of Engineering, Atilim University, 06836 Ankara, Turkey
[c]Metallurgical and Materials Engineering Department, Marmara University, 34722 Istanbul, Turkey

Received 18 March 2013; received in revised form 11 April 2013; accepted 15 April 2013
Available online 24 April 2013

Abstract

In this article, the yttrium solubility effects on the structural, dielectric and optical properties of the $Bi_{1.5-x}Y_xZn_{0.92}Nb_{1.5}O_{6.92}$ (Y–BZN) solid solutions are investigated. The yttrium content (x) was varied in the range of 0.04–0.6. The scanning electron microscopy and energy dispersion analysis have shown that the single phase of the yttrium doped pyrochlore is possible up to yttrium content of 0.06. At $x=0.07$ $YNbO_4$ minor phase appears and at $x=0.08$ $YNbO_4$ and ZnO dominates in the Y–BZN. Due to the very rare amount and the random distribution of the minor phases in the pyrochlore, the X-ray diffraction technique was not able to detect these minor phases at low yttrium doping levels. While the nonstoichiometric phase evaluated at $x=0.07$ displayed no role on the relative density, the dielectric constant, dielectric loss, the temperature coefficient of dielectric constant, the absorbance and the energy band gap are observed to be sharply altered. The energy band gap of the pure BZN widened from 3.30 eV to 3.60 eV when the BZN was doped with Y content of 0.04. It then sharply shrunk to 2.75 eV for Y content of 0.07.

Keywords: Yttrium doping; Transmittance; Energy gap; Dielectric constant

1. Introduction

Bismuth niobium zinc oxide (BZN) pyrochlore ceramics are now in the focus of researchers due to their astonishing electronic applications. Tunable coplanar waveguide line made of bismuth zinc niobate thin films have been successfully fabricated and evaluated in the range from 0 to 10 GHz by measuring the scattering parameters on a probe station [1]. The device responded finely as low-voltage phase shifter. At low electric field and at a frequency of 10 GHz the phase difference was 10°. In addition, tunable parallel-plate capacitors that employ $Bi_{1.5}Zn_{1.0}Nb_{1.5}O_7/Ba_{0.5}Sr_{0.5}TiO_3$ (BZN/BST) thin films for RF applications are also reported to exhibit large tunability of 39% at 40 V and high device quality factor of 300 at 1 MHz [2]. This device has low leakage current density even under a high applied bias. In an earlier study, Lee et al. reported the design of very high tunable inter-digital capacitor (IDC) using the bismuth zinc niobate (BZN) pyrochlore thin-film dielectrics. The device was tested for microwave applications. The BZN increased the tunability of the IDC and reduced DC bias voltage. At a DC voltage biasing of 20 V the IDC yielded a tenability of 72 and 75% for signal frequencies of 2.4 and 5.8 GHz, respectively [3].

Literature data reports various types of studies on the BZN pyrochlore. One of most interesting works is the purposely doping of the BZN ceramics. As for example, doping of CuO into the BZN lowered the sintering temperature significantly [4]. Similarly, vanadium metal which was doped into the $Bi_{1.5}Zn_{1.0}Nb_{1.5}O_7$ pyrochlore as sintering aid lowered the sintering temperature to 850 °C [5]. In addition, Ti doped $Bi_{1.5}Zn_{1.0}Nb_{1.5}O_7$ pyrochlore ceramics [6] are observed to exhibit significant increase in the dielectric constant via increasing the Ti content. Moreover, Gd incorporation into the A-site of $Bi_{1.5}Zn_{1.0}Nb_{1.5}O_7$ pyrochlore instead of Bi significantly altered the dielectric properties [7].

In this article we will discuss the pronounced changes in the structural, dielectric and optical properties of the BZN system

*Corresponding author at: Group of Physics, Faculty of Engineering, Atilim University, 06836 Ankara, Turkey. Tel.: +972 599379412; fax: +970 42510810x817.
E-mail addresses: aqasrawi@atilim.edu.tr, aqasrawi@aauj.edu (A.F. Qasrawi).

0272-8842/$ - see front matter © 2013 Elsevier Ltd and Techna Group S.r.l. All rights reserved.
http://dx.doi.org/10.1016/j.ceramint.2013.04.050

via yttrium doping. Particularly, these physical characteristics will be studied, analyzed and compared below and above the solubility limit of the yttrium in the pyrochlore. The work which will be investigated for the first time aims to provide an idea about the applicability of BZN ceramics at high frequency ranges.

2. Experimental details

Powder samples having the formula $Bi_{1.5-x}Y_xZn_{0.92}Nb_{1.5}O_{6.92}$ with x being in the range of 0.04–0.6 were prepared by the conventional high temperature solid state reaction technique using stoichiometric mixture of Bi_2O_3 (99.99%, Aldrich), Nb_2O_5 (99.5%, Merck), ZnO (99.5%, Aldrich) and Y_2O_3 (99.9%, Alfa Aesar). After mixing the powders by ball milling for 15 h in ethanol using zirconia balls, they were dried and calcined at 800 °C for 4 h. The calcined powders were milled in an agate mortar and then pressed into disks with ~0.076 cm thickness and 1.0 cm diameter. The doped pellets were sintered at 1100 °C for 4 h, in a tightly closed alumina crucible to prevent evaporation losses. The densities of the samples were measured by Archimedes method. The microstructure of the sintered samples was investigated using scanning electron microscope JEOL JSM 5600 LV. X-ray diffraction analysis was performed using an X-ray diffractometer (Rigaku, Cu K_α radiation, 18/min) using powdered samples and the unit cell parameters were computed by the least square method. The electrical contacts to the samples were made by evaporating silver onto the sample surface using, Edwards Auto 500. The dielectric constant and dielectric loss measurements were carried out using HP 4284A LCR meter at room and at 200 °C temperatures. The optical transmittance and reflectance was measured in the incident light wavelength range of 200–1100 nm using Evolution 300 spectrophotometer with VeeMax II variable angle reflectometer attached to the spectrophotometer.

3. Results and discussion

The yttrium doping effects on the structural properties of the $Bi_{1.5}Zn_{0.92}Nb_{1.5}O_{6.92}$ pyrochlore ceramics was carried out by means of scanning electron microscopy (SEM) and X-ray diffraction techniques. The stoichiometric compositional analysis in accordance to the empirical formula $Bi_{1.5-x}Y_xZn_{0.92}Nb_{1.5}O_{6.92}$ was also done by means of energy dispersive X-ray spectroscopy attached to the system (EDS). In the current work, the yttrium content (x) was varied from 0.04 to 0.10 in 0.02 incremental steps and from 0.10 to 0.60 in 0.10 incremental steps. Fig. 1(a) and (b) displays the SEM images for the yttrium content of 0.06. The presentation in Fig. 1(a) and (b) relate to secondary electron images (SEI) being registered at 2000 and 10,000 enlargement scales. The estimated grain size is ~7.0–8.0 μm. For this sample, the EDS analysis reflected stoichiometric composition consistent with the single phase pyrochlore. On the other hand Fig. 2(a) and (b) illustrates the SEM images for the samples with 0.08 yttrium content. The back scattered electron images (BEI) which relates to a 500 enlargement indicated the appearance of a strange area in the structure. This region appears better in Fig. 2(b) which reflects BEI images for 1000 enlargement. It is assigned as point 1 in the same image. Another two points assigned as point 2 and 3 are also selected for the purpose of compositional analysis. Similarly, the SEI images presented in Fig. 2(c) and (d) reflect the same observation for the enlargements of 2000 and 10,000, respectively. The estimated average grain size for this sample as apparent from Fig. 2(c) is ~11 μm. The EDS analysis of the points 1, 2 and 3 are displayed in Fig. 3(a), (b) and (c), respectively. The dispersive energy spectra of point 1 relates to $YNbO_4$ as minor phase but EDS spectra are also coming from BZN grains around this second phase. On the other hand, while point 2 presents the single phase doped pyrochlore, point 3 indicated the existence of ZnO phase in the studied samples.

In order to determine the solubility limit of the $Bi_{1.5-x}Y_xZn_{0.92}Nb_{1.5}O_{6.92}$ pyrochlore, new samples with 0.07 yttrium content were prepared and tested. The images for this sample are shown in Fig. 4. The points 1 and 2 displayed in Fig. 4(b) reflected an EDS spectrum similar to those displayed in Fig. 3 (a) and (b), respectively. The EDS analysis for the 0.07 doping ratio reflected the existence of $YNbO_4$ at the grain boundaries of the BZN and the ZnO phase was absent. Although the images displayed less amount of $YNbO_4$ compared to the samples which contains 0.08 yttrium, it still assures that the solution limit for this pyrochlore is at $x=0.06$. The average grain size for the 0.07 yttrium doped samples was also ~11 μm.

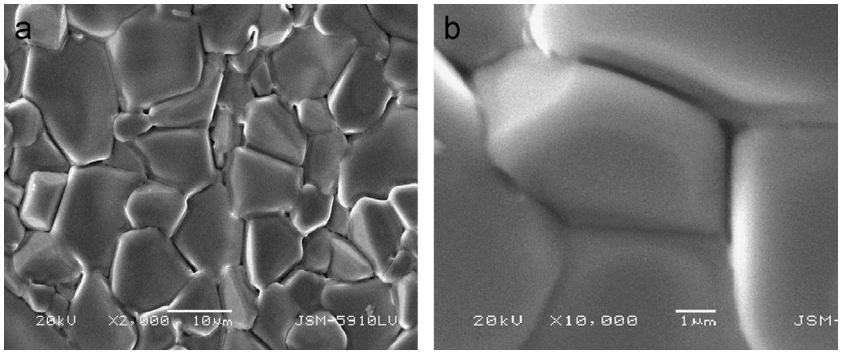

Fig. 1. The SEM images for the $Bi_{1.42}Y_{0.06}Zn_{0.92}Nb_{1.5}O_{6.92}$ solid solution being synthesized at 1100 °C for 4 h. (a) 2000 enlargement and (b) 10,000 enlargement of SEI images.

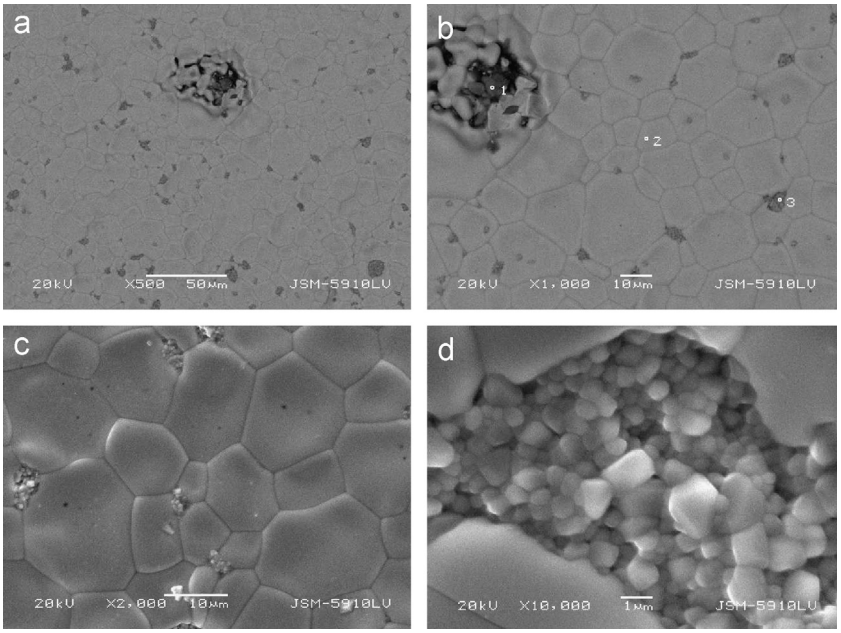

Fig. 2. The images of the $Bi_{1.42}Y_{0.08}Zn_{0.92}Nb_{1.5}O_{6.92}$ solid solution being synthesized at 1100 °C for 4 h. (a) The BEI images for enlargement of 500 times and (b) for BEI 1000 enlargement. (c) The SEI image for a 2000 enlargement and (d) the SEI image at 10,000 enlargement.

Fig. 5 displays the X-ray diffraction results for the investigated samples. As it is readable from the figure, single phase of the yttrium doped pyrochlore was observed up to a doping content of 0.07. In contrast to the SEM results, the X-ray diffraction patterns of the 0.07 doped samples did not reflect any extra intensity of the minor phases. The inability of the X-ray diffraction to display the observed minor phase of the $YNbO_4$ may be ascribed to the very little amount of the phase and may also be due to the random distribution of the $YNbO_4$ grains through the pyrochlore. The X-ray diffraction patterns of the sample doped with 0.08 is consistent with that shown in Fig. 2 but with the absence of ZnO minor phase. The appearance of the $YNbO_4$ phase at this level of doping is attributed to the increase in it's amount through the pyrochlore. On the other hand, for the same reasons, the ZnO phase appears only at doping levels of yttrium being greater than 0.08.

Unfortunately, up to our knowledge, the yttrium solubility in the BZN pyrochlore ceramics is not investigated yet. Thus, comparison with similar work is not possible at the current stage. In our previous works we have reported and discussed the solubility of Sm, Nd and Fe in the BZN pyrochlore in accordance to the empirical formulae $Bi_{1.5-x}Sm_xZn_{0.92}Nb_{1.5}O_{6.92}$, $Bi_{1.5-x}Nb_xZn_{0.92}Nb_{1.5}O_{6.92}$ and $Bi_{1.5}Zn_{0.92}Nb_{1.5-x}Fe_xO_{6.92-x}$, respectively. The respective solubility limits of these cations were determined as $x=0.13$, 0.18 and 0.15 [8]. In another work we have shown that the solubility of the doping agent depends mainly on the sites of the atomic substitution [9]. Namely, when tin atoms was substituted in the A $(Bi_{1.5}Zn_{0.46})$-site instead of zinc and in the B $((Zn_{0.46}Nb_{1.5})$-site instead of niobium in accordance to the chemical formulae $Bi_{1.5}Zn_{0.92}Nb_{1.5-x}Sn_xO_{6.92-x/2}$ and $(Bi_{1.5-x/3}Zn_{0.46-3x/2}Sn_x)(Nb_{1.5}Zn_{0.46})O_{6.92}$, for $0.00\leq x\leq 0.40$ and $0.00\leq x\leq 0.60$, respectively. The relative solubility limits was possible for x values less than 0.25 and less than 0.10.

The yttrium solubility limit is observed to exhibit pronounced effect on the physical properties of the $Bi_{1.5-x}Y_xZn_{0.92}Nb_{1.5}O_{6.92}$ ceramics. Particularly, for the samples which were sintered to obtain high density pellets at sintering temperature of 1100 °C, the average theoretical, bulk and relative densities for yttrium content of 0.04, and 0.07 was 7.05 and 7.02 and 6.88 and 6.83 (g/cm^3) and 97.58% and 97.29%, respectively. This data indicates that the existence of the minor phase of $YNbO_4$ in the 0.07 doped samples does not affect the pyrochlore density. On the other hand, the room temperature dielectric constant and the loss tangent of the dielectric which were recorded at 1.0 MHz exhibited values of 147 and 136 and 0.0015 and 0.0026 for Y content of 0.04 and 0.07, respectively. The respective temperature coefficient of dielectric constant,α_ε, which was calculated from the relation $\alpha_\varepsilon=(\varepsilon_{T2}-\varepsilon_{T1})/(\varepsilon_{T1}(T_2-T_1))$ with $T_1=298$ K and $T_2=393$, exhibited values of -497 ppm/°C and -600 ppm/°C. The dielectric constant values recoded for the Y-doped BZN is lower than those which we have previously observed for Sn doped BZN. The dielectric constant for the Sn doped BZN was observed to be ~266 when Sn replaces Nb and 167 when Sn replaces Zn [9]. The dielectric constant values reported for Y-doped BZN are comparable to those of Sm doped with Sm content of 0.05 and 0.07 and less than those reported for Fe content of similar ratios [8].

In order to investigate the optical properties, the room temperature transmittance (T) and reflectance (R) of the samples were recorded in the spectral wavelength range of 200–1100 nm. The experimental data are used to calculate the optical absorption coefficient (α) through the relation, $T=(1-R)^2\exp(-\alpha d)$with d~0.076 cm being the thickness

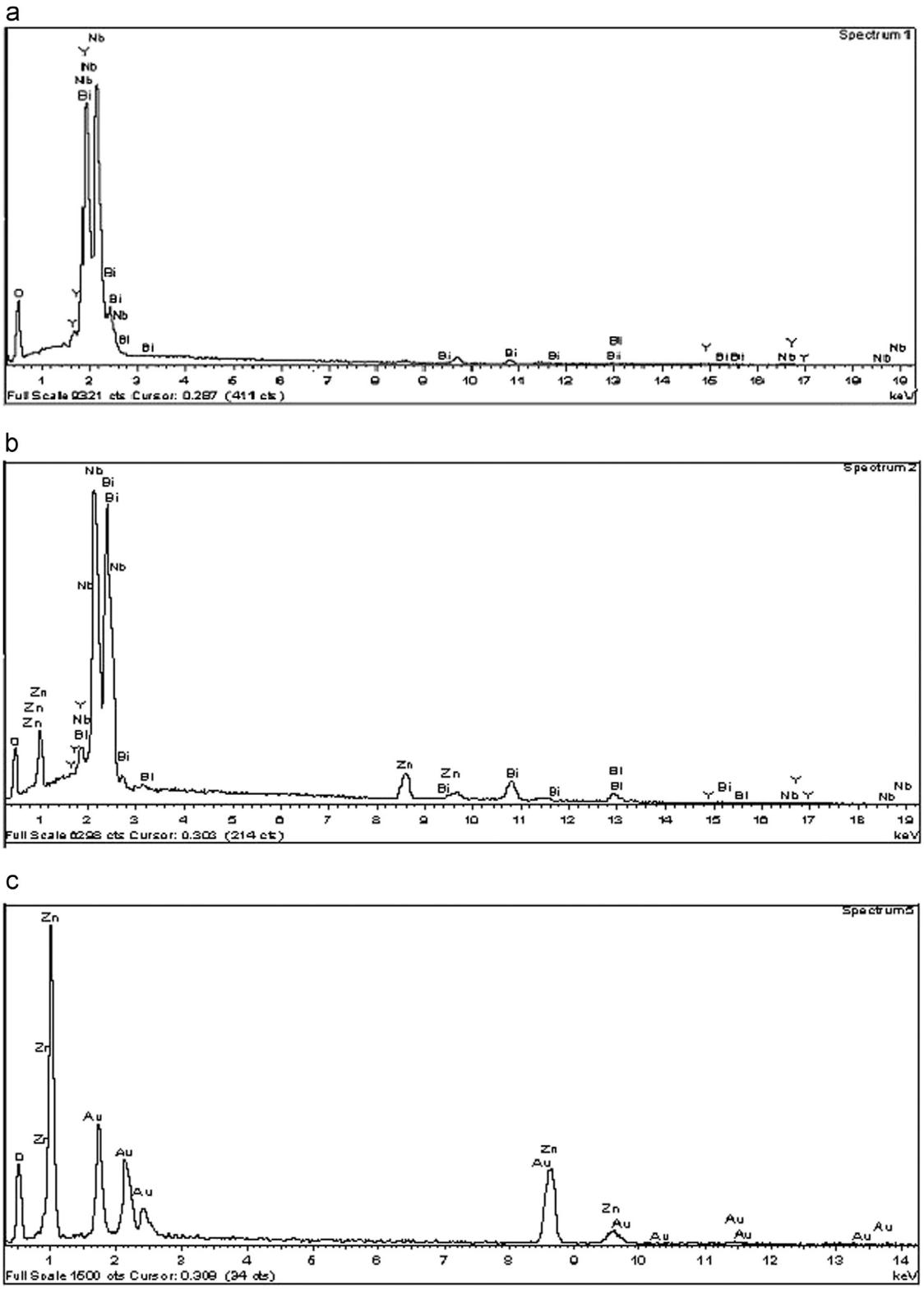

Fig. 3. The compositional analysis for (a) point 1, (b) point 2 and (c) point 3 of $Bi_{1.42}Y_{0.08}Zn_{0.92}Nb_{1.5}O_{6.92}$ which is displayed in Fig. 2(b).

for both samples. The absorption spectra are illustrated in Fig. 6(a). The figure reflects a sharp decrease in α values with decreasing incident photon energy down to 4.82 eV. Below 4.82 eV, it tends to remain constant over all the studied range of energy. It is also readable from the figure that although both samples are of the same thickness, the absorption coefficient values are larger for the samples doped with 0.07 yttrium than those doped with 0.04. The non-vanishing absorption coefficient indicates the existence on interband transitions in the material. The non-vanishing absorption coefficient in the

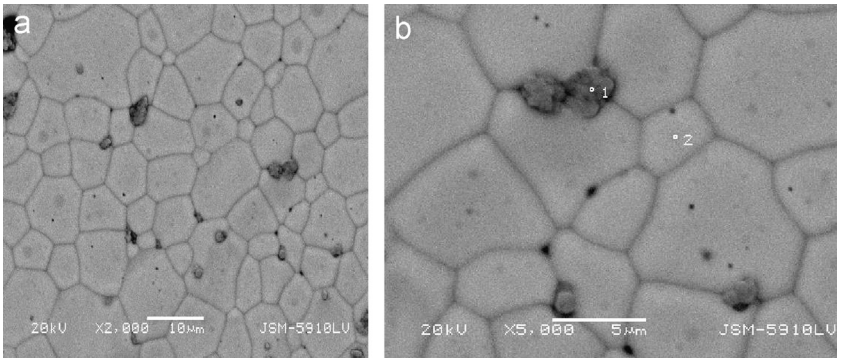

Fig. 4. The images of the $Bi_{1.42}Y_{0.07}Zn_{0.92}Nb_{1.5}O_{6.92}$ solid solution being synthesized at 1100 °C for 4 h. (a) The BEI images for enlargement of 2000 times and (b) for BEI 5000 enlargement. (Point 1 and 2 shown in (b) are $YNbO_4$ and BZN pyrochlore, respectively).

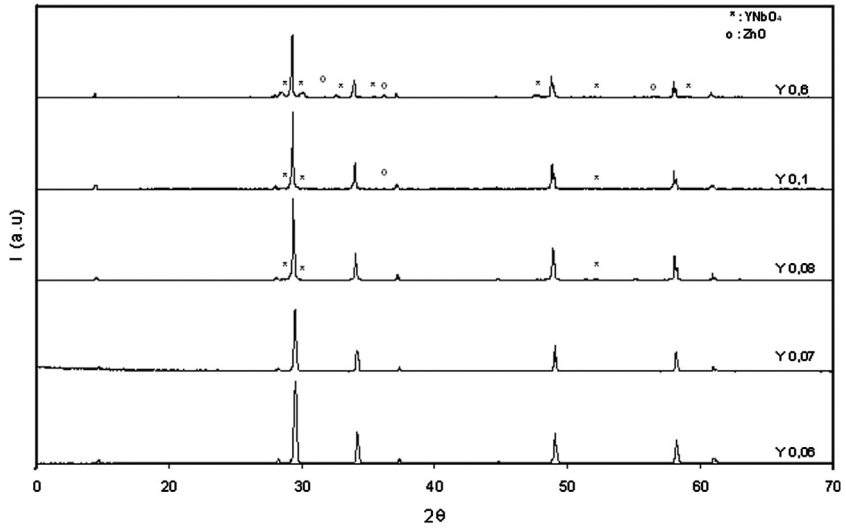

Fig. 5. The X-ray diffraction patterns for $Bi_{1.5-x}Y_xZn_{0.92}Nb_{1.5}O_{6.92}$ pyrochlore ceramics.

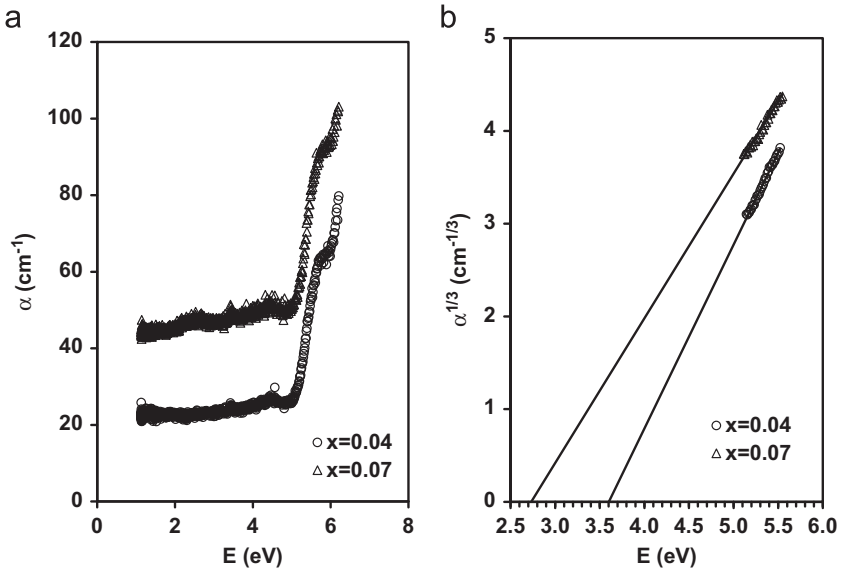

Fig. 6. (a) The absorption coefficient spectra and (b) the $\alpha^{1/3}-E$ for $Bi_{1.5-x}Y_xZn_{0.92}Nb_{1.5}O_{6.92}$ pyrochlore ceramics.

transparent region of the Y-doped pyrochlore was also observed for pure [9] and Ni doped [10] BZN pyrochlores. The interband transitions can be ascribed to the existence of the defects that introduces alternative energy levels between the intrinsic bands and as a result subsequently reduces the band gap [11]. Similarly, the attenuation in the absorption

coefficient via the appearance of multiphase in the Y-doped pyrochlore is attributed to the same reasons.

Attenuations of interband transitions are reported to be sensitive to the elemental composition of the single and multiphase materials. **Aouadi** et al. [12] studied the changes in the optical properties of the single phase $Ta_{1-x}Zr_xN$ and the multiphase of ZrN–Ag films. They observed that the energy of the interband transition can be altered by any changes in the elemental composition for single phase materials. For multiphase structures, the strength and width of the interband transition were also reported to be attenuated to reflect the changes in phase composition and microstructure.

The spectra of the absorption coefficients are analyzed in the light of our previous investigations on Ni doped BZN [10]. Namely, in the strong absorption region, the absorption coefficient spectra follow the equation, $\alpha^{1/3} = B(E-E_g)$, with B being a constant that depends on the transition probability, E is the energy of incident photons and E_g is the energy band gap of the yttrium doped pyrochlore. The linear solid lines presented in Fig. 6(b) which are the fittings of the experimental data shown as open circles for $x=0.04$ and open triangles for $x=0.07$ Y-content, represent the indirect forbidden electronic transitions from the valance to the conduction band of the $Bi_{1.5-x}Y_xZn_{0.92}Nb_{1.5}O_{6.92}$ solid solution. As the figure shows, the E-axis crossing is located at 3.60 and 2.75 eV for the samples doped with 0.04 and 0.07, respectively. The numerical values of the energy gap reflects a sharp increase from 3.30 eV for the pure samples [10] to 3.60 for $x=0.04$ of Y doping and sharp decrease to 2.75 eV when yttrium content was increased to 0.07. The increase in the energy band gap of the pure sample from 3.30 to 3.60 eV via 0.04 yttrium content substitution is similar to those which we have previously observed for Ni doping [10] and is assigned to the structural modifications associated with the atomic substitutions.

As it is also seen from the above data when the yttrium content increased from 0.04 to 0.07, the energy band gap drastically decreases from 3.60 to 2.75 eV. This remarkable decrease is probably due to the creation of sub-band gaps in the material due to the minor phase $YNbO_4$ which exists in the 0.07 Y-doped samples. In addition, the increase in the free carrier density due to the increasing Y-content may have caused the energy band gap narrowing. An important note to view here is the work of Yogamalar et al. who have studied the dopant induced band gap narrowing in Y-doped zinc oxide nanostructures [13] and reported that the yttrium dopant ions stabilizes in wurtzite hexagonal phase of ZnO up to the concentration of less than 6 at% and ascribed this behavior to the fact that the ZnO lattice expands and the optical band gap energy decreases at this level. They also abstracted that increasing the dopant concentration to values greater than 6 at% leads to a contraction of the ZnO lattice, which in turn produces a significant structural disorder observed from the shift in the XRD peaks due to additional interstitial incorporation of Y. Although the ZnO minor phase is still not apparent in the samples which contain an amount of 0.07-yttrium, such reaction between the Zn, O and Y atoms (composers of the $Bi_{1.5-x}Y_xZn_{0.92}Nb_{1.5}O_{6.92}$ pyrochlore ceramics) may be one of the reasons for the band gap narrowing.

4. Conclusion

The yttrium doping effects on the structural, dielectric and optical properties of the BZN are investigated and discussed. The Y-doped BZN exhibit single phase of the pyrochlore for yttrium content less than 0.07. Further increase in the doping agent cause a structure disorder associated with the domination of the $YNbO_4$ and ZnO minor phases in the pyrochlore. While the effect of structure disorder on the mass density is less pronounced, it reduces the values of the dielectric constant and the energy band gap from 147 and 3.60 eV to 136 and 2.75 eV, respectively.

Acknowledgments

The authors would like to submit their thanks to the scientific and technological research council of Turkey (TÜBİTAK) and to the scientific research committee of Arab-American University (AAUJ) at Palestine for the financial support. The work was supported by the TÜBİTAK under the Project 107M083 and by the AAUJ under the Project code (2011-2012 Cycle I).

References

[1] Y.C. Lee, K.H. Ko, Tunable coplanar waveguide (cpw) line integrating bismuth zinc niobate (BZN) thin films, Progress in Electromagnetics Research Letters 19 (2010) 75–82.
[2] R. Li, S. Jiang, L. Gao, L. Wang, Y. Li, Tunable capacitors employing BZN/BST thin films for RF applications, IEEE Transactions on Ultrasonics, Ferroelectrics and Frequency Control 58 (2011) 1140–1144.
[3] Y.C. Lee, Y.P. Hong, D.M. Kim, K.H. Ko, Very high tunable interdigital capacitor using bismuth zinc niobate thin-film dielectrics for microwave applications, Electronics Letters 42 (2006) 851–853.
[4] M.-C. Wu, Y.-C. Huang, W.-F. Su, Silver cofirable $Bi_{1.5}Zn_{0.92}Nb_{1.5}O_{6.92}$ microwave ceramics containing CuO-based dopants, Materials Chemistry and Physics 100 (2006) 391–394.
[5] D. Huiling, Y. Xi, Dielectric relaxation characteristics of bismuth zinc niobate pyrochlores containing titanium, Physica B 324 (2002) 121–126.
[6] W.F. Su, S.C. Lin, Interfacial behaviour between $Bi_{1.5}ZnNb_{1.5}O_7 \cdot 0.02V_2O_5$ and Ag, Journal of the European Ceramic Society 23 (2003) 2593–2596.
[7] M. Valant, P.K. Davies, Crystal chemistry and dielectric properties of chemically substituted $(Bi_{1.5}Zn_{1.0}Nb_{1.5})O_7$ and $Bi_2(Zn_{2/3}Nb_{4/3})O_7$ pyrochlores, Journal of the American Ceramic Society 83 (2000) 147–153.
[8] A. Mergen, H. Zorlu, M. Ozdemir, M. Yumak, Dielectric properties of Sm, Nd and Fe doped $Bi_{1.5}Zn_{0.92}Nb_{1.5}O_{6.92}$ pyrochlores, Ceramics International 37 (2011) 37–42.
[9] A.F. Qasrawi, Hussein A. Abu Je'ib, A. Mergen, Effect of ionic substitution on the structural, dielectric and electrical properties of bismuth zinc niobate ceramics, Journal of Ceramic Processing Research 13 (2012) 446–450;
A.F. Qasrawi, A. Mergen, Journal of Alloys and Compounds 496 (2010) 87–90.
[10] A.F. Qasrawi, E.M. Nazzal, A. Mergen, Advanced Applied Ceramics 111 (2012) 165–170.
[11] S. Chang, R. Doong, Interband transitions in sol–gel-derived ZrO_2 films under different calcination conditions, Chemistry of Materials 19 (2007) 4804–4810.
[12] S.M. Aouadi, A. Bohnhoff, T. Amriou, M. Williams, J.N. Hilfiker, N. Singh, J.A. Woollam, Vacuum ultra-violet spectroscopic ellipsometry study of single- and multi-phase nitride protective films, Journal of Physics: Condensed Matter 18 (2006) S1691–S1701.
[13] R. Yogamalar, P.S. Venkateswaran, M.R. Benzigar, K. Ariga, A. Vinu, A.C. Bose, Dopant induced band gap narrowing in Y-doped zinc oxide nanostructures, Journal of Nanoscience and Nanotechnology 1 (2012) 75–83.